Pergamon

0301-9322(94)00065-4

Int. J. Multiphase Flow Vol. 21, No. 2, pp. 305–313, 1995

0301-9322/95 $9.50 + 0.00

BRIEF COMMUNICATION

THE EXTENT OF THE BUBBLE-DEPLETED REGION IN THE FRONTAL VICINITY OF A LARGE CAP BUBBLE RISING IN A BUBBLE SWARM

K. TSUCHIYA†, K. OHSAKI and K. TAGUCHI
Department of Chemical Science and Technology, The University of Tokushima, Tokushima 770, Japan

(Received 2 May 1994; in revised form 20 September 1994)

INTRODUCTION

Bubble columns have been widely used as gas–liquid(–solid) contacting devices such as gas absorbers and/or strippers, chemical reactors for hydrogenation, oxidation or chlorination of organic liquids, direct/indirect coal liquefaction and Fischer–Tropsch synthesis, fermenters and biological wastewater treatment units. Such a diversity of applications reflects a wide range of operating conditions which should be incorporated into the evaluation or prediction of column performance. The hydrodynamics of the bubble columns which predominate the mass and heat transfer characteristics of the system are still not fully understood due to the extreme complexity of the bubble flow structure.

The complex behavior of the bubble swarms mainly stems from the broad distribution (local non-uniformity) of the bubble rise characteristics such as bubble size, bubble rise velocity and gas hold-up throughout the column. Under limited operating conditions, the bubble flow exhibits a relatively simple structure; the so-called homogeneous/uniform-bubbling regime occurs when a swarm of small bubbles is evenly dispersed at low gas velocities. Such an "ideal" regime, however, is rarely met in the practical operation of industrial bubble column reactors (BCRs); non-uniformity, or the presence of large bubbles, is inevitable and needs to be taken into account in reactor design and operation. One of the important features in this heterogeneous (or so-called churn-turbulent) regime is the interaction between the large bubbles and the surrounding small bubbles.

Investigations specifically concerning the interaction between large and small bubbles are not so extensive in the literature. Hills (1975) appears to be the first to study, though in a two-dimensional system, the influence of a swarm of small bubbles on the rise of a large bubble, which he referred to as a "cap" to distinguish it from each "bubble" constituting the swarm—the same convention applies in this study. Hills' analyses were limited to predicting the trajectories of the individual bubbles overtaken by a cap in swarms of low gas hold-ups, thus in the absence of direct cap–bubble interactions. His important findings are: (1) that a "hole" exists in the swarm which Hills designated as a region of negligible bubble population immediately ahead of the cap frontal surface—to be called the "bubble-depleted" region in this study—predicted theoretically and confirmed experimentally; (2) at high swarm gas hold-ups (>4%), marked concentrations of bubbles appear around this region, whose size in this case diminishes, which promotes bubble coalescence and thus the formation of secondary "satellite caps", which then rise in the wake of the primary cap and coalesce with it.

Besides the work of Hills (1975) just described, most efforts have been directed towards studying the enhancement of the cap rise velocity in the presence of the surrounding bubbles. Hills & Darton (1976) continued Hills' study, in both two- and three-dimensional columns, to elucidate the

†To whom correspondence should be addressed.

mechanism for this enhancement effect. Their conclusion was that enhancement is not necessarily due to "gulf-stream" circulation of the liquid phase nor to bubble coalescence, but probably results from small-scale turbulent eddies in the liquid phase generated by the swarm bubbles. This latter contribution tends to distort the frontal surface of the cap thereby altering the liquid flow pattern around the cap nose. Miyahara & Fan (1992) conducted a similar study in the gas–liquid–solid fluidized bed. Their major finding was that the extent of enhancement of the cap bubble velocity can be estimated by applying the concept of "wake velocity"—in essence, the contribution of the liquid circulation induced by the bubble swarm—for in-line caps (Marks 1973; Miyahara *et al.* 1991).

The present study concerns the visual observation of the formation of the bubble-depleted region in the frontal vicinity of a large bubble injected into a swarm of otherwise uniformly dispersed small bubbles. For this purpose, experiments are conducted exclusively in a two-dimensional column to ensure the distinct appearance of a single cap throughout its rise in the swarm over a wide range of gas hold-ups. Other parameters, including physical properties of the gas and liquid phases and sizes of the two classes of bubbles, are either fixed or of limited ranges. The specific focus is on the measurement of the size of the bubble-depleted region.

EXPERIMENTAL

Figure 1 shows a schematic diagram of the experimental set-up used in this study. The two-dimensional column is made of transparent PVC and has a main section of 1.0 m effective height, 0.218 m width and 10 mm gap thickness. Below this section is the gas-distributing section which consists of a gas chamber of five isolated, equal-sized compartments and a 5 mm thick PMMA porous plate of 30 μm pore size and 35% porosity (Spacy Chemical Inc., Tokyo) fixed separately above each compartment. The total gas flow into the column is controlled by the orifice flow meter; the gas flow through each compartment is individually regulated by a needle valve so as to attain an even distribution of gas flow, i.e. a uniform swarm of small bubbles throughout the column.

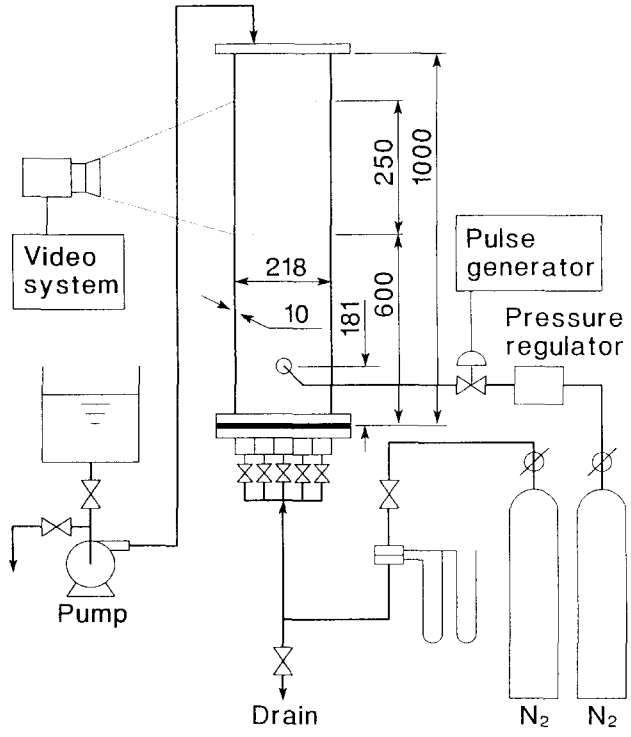

Figure 1. Schematic diagram of the experimental set-up.

A separate gas injection is made through a 4.0 mm i.d. (1.0 mm thick) stainless steel nozzle, with a tapered (to o.d.) outlet, flush-mounted on the rear wall at a distance of 181 mm above the top of the gas-distributing section. A single, large/cap bubble with no satellites can be readily generated; the bubble size is controlled roughly by altering the opening time of the solenoid valve, which is regulated by an electric pulse-signal generator, and precisely by regulating the gas delivery pressure with the digital pressure gauge of ± 10 Pa precision.

A video camera system is utilized to obtain: (1) the rise characteristics of each cap, including the rise velocity and the shape/dimensions [mainly the major axis (breadth) and minor axis (height)]; (2) the state of redispersion of the swarm bubbles around the "disturbing" cap and, more specifically, the extent (characteristic length or effective area) of the bubble-depleted region in the frontal vicinity of the cap surface; and (3) the fate (i.e. shape distortion or breakup) of the cap under the influence, directly or indirectly, of the interacting swarm bubbles. The video camera is fixed at a location 0.725 m above the gas distributor so as to obtain an effective observation zone spanning a vertical distance between 0.60 and 0.85 m. The cap rise characteristics are measured by analyzing frame-by-frame the recorded video images, all of which are obtained over an exposure time of 1/1000 s at 30 frames/s. Under each experimental condition (with at least 100 cap injections), the average size of the bubble-depleted region is determined from selected (neither disintegrated nor severely distorted) caps—ten or more depending on the swarm gas hold-up—at four instances/frame for each cap. The specific procedure, including the precise definition of the bubble-depleted region, is described in the ensuing section. As an auxiliary observation, the cap–bubble interactions are closely monitored via the video system, which is helpful in improving our understanding of the role of the bubble-depleted region in the complex behavior of heterogeneous bubble swarms.

Nitrogen is used as the gas phase for both the swarm and the cap bubbles; tap water is used as the liquid phase, which is initially fed to the column via a pump and is kept batchwise during each run. The swarm gas hold-up is estimated based on the conventional method of measuring the aerated and unaerated liquid levels (and thus their difference) for each superficial gas velocity tested over the range 0–0.02 m/s. The size distribution of the swarm bubbles is determined from focused video images by measuring the maximum and minimum dimensions scaled on the images for at least 100 bubbles under each condition. Since the minor axis of a wobbling bubble is not necessarily vertically oriented, the sizes of the individual bubbles are represented in this study, for simplicity, by the arithmetic mean of the two dimensions, as suggested by Akita & Yoshida (1974). To assure reasonable distinction between the two classes of bubbles, i.e. the swarm bubbles and caps, when they coexist, and at the same time to avoid any excess destabilization of the caps and excess wall effects caused by the side walls, the size of the single caps in this study is fixed at 28.4 ± 1.6 mm breadth (b). All the experiments are conducted at a temperature range of 22 ± 2°C.

RESULTS AND DISCUSSION

Characteristics of swarm bubbles and their influence on the formation of the bubble-depleted region

In a bubble swarm of very low gas hold-up, individual bubbles behave as if they were isolated. As the gas hold-up (ϵ_G) increases, each bubble begins to "feel" the existence of its neighbors; the interaction between the bubbles in this state tends to reduce the apparent bubble rise velocity—hindered rising. The rise velocity of the individual bubbles (u_s) is uniform in an ideal dispersion and, based on the drift–flux concept (e.g. Wallis 1969), is generally described by the expression:

$$u_s = U_G/\epsilon_G = U_b(1-\epsilon_G)^{n-1} \qquad [1]$$

where u_s is defined as the relative velocity between the interstitial gas and liquid velocities (the latter being zero in this study of a batch-liquid system); U_G is the superficial gas velocity and U_b the terminal rise velocity of an isolated bubble representative of the swarm bubbles; n is an empirical parameter with suggested values ranging from 1 to 2.4.

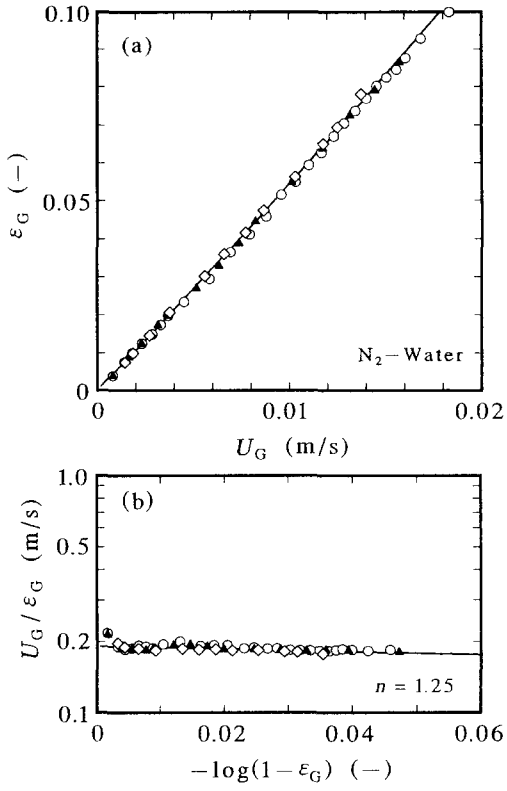

Figure 2. Relationship between swarm gas hold-up and superficial gas velocity in terms of (a) direct and (b) drift–flux plots. The different symbols correspond to different runs signifying the reproducibility of the data.

Figure 2 presents typical plots of (a) the conventional ϵ_G–U_G and (b) the drift–flux (i.e. [1]) relationships. The solid line, obtained in figure 2(b) by curve-fitting [1] to the present experimental data (thus incorporating the 2-D wall effects associated with the front and rear walls on the two parameters, U_b and n), bounds the upper limit of ϵ_G; the best fit gives $U_b = 0.19$ m/s—the asymptotic value of U_G/ϵ_G as $\epsilon_G \to 0$—and $n = 1.25$—indicating a slight hindrance effect. Departure of the experimental data from the line representing [1] occurs as ϵ_G exceeds 0.08, beyond which uniform bubbling breaks down and clustering or eventual coalescence among the swarm bubbles begins to predominate (Tsuchiya & Nakanishi 1992). In the present study only the conditions for uniform bubbling thus confirmed are utilized in generating the "background" swarm.

The size distribution of swarm bubbles is found to be rather narrow under each hold-up condition; mean bubble sizes with standard deviations were 2.28 ± 0.42, 3.20 ± 0.58, 3.99 ± 0.75 and 4.16 ± 0.73 mm at $\epsilon_G = 0.0046$, 0.0169, 0.0400 and 0.0599, respectively, where the simple arithmetic mean is considered to be sufficient for the present purpose of identifying the representative bubble sizes. While varying their (equivalent) diameters from 2.3 to 4.2 mm, these representative bubbles, with negligible to moderate bubble–bubble interaction, are known to possess almost an identical rise velocity of ~0.22–0.23 m/s in three dimensions (Clift *et al.* 1978) and, in the present 2-D system, ~0.18–0.19 m/s [not measured directly but estimated as in figure 2(b)].

The bubble size and gas hold-up for swarm bubbles are two important parameters, besides the cap rise properties which are fixed in this study, affecting the extent as well as the formation of the bubble-depleted region. This region, on a speculative basis, arises from the modification—due to the presence of the cap—of the hydrostatic pressure gradient in the absence of the cap, the consequence of which is interpreted as a local variation/increase in the effective buoyancy acting on the swarm bubbles being overtaken by the cap; the bubble rise velocity increases as the vertical distance between the bubble and the cap decreases and, under sufficient pressure gradient, reaches

the cap rise velocity. When this limiting state is attained before the bubbles (strictly speaking, ones along the central axis of the cap rise) have been overtaken by the cap, there remains a finite bubble–cap distance which is a measure of the extent of the bubble-depleted region. While the bubble rise velocity is generally a function of bubble size, it remains almost constant or only varies slightly with the gas hold-up [see figure 2(b)] in the present case—thus rendering the influence of bubble size minimal. However, when the swarm bubble population is sufficiently small (i.e. at low ϵ_G), the chances for the bubbles along or very close to the cap central axis to escape under an ever-increasing pressure gradient even before the limiting state is reached, can become substantial, thus increasing the effective bubble–cap distance. No further attempt is made to predict the extent of the bubble-depleted region based on the above physical scenario, which is beyond the scope of the present communication; only experimental evidence regarding the measure of the pertinent region and the gas hold-up effect is presented in the following.

Definition and estimation procedure of the extent of the bubble-depleted region

Figure 3 gives a sketch, taken directly from one frame of the video image, of the swarm bubbles redispersed by the approaching cap at an intermediate ϵ_G ($=0.032$) investigated in this study ($\epsilon_G = 0$–0.06); a tracing is made mainly above the (nearly horizontal) baseline passing approximately adjacent to the cap edges. Note that demarcation can be identified between the region of no bubbles, i.e. the bubble-depleted region (or layer), in the frontal vicinity of the cap and the surrounding region of higher bubble concentration. Similar bubble-population distributions are found under other conditions, though with slightly vague—but still clear enough for the present objective—demarcations of the boundary at a lower ϵ_G (<0.01). In the sketch the cap appears not to be too distorted from the inherent circular-cap shape (with round edges).

Also given in figure 3 are the supplemental lines drawn for estimating the extent of the bubble-depleted region. A simple approach is taken in this study where seven lines, numbered $i = -3$ to 3 and emanating from the center of the cap base, are equally spaced (by 30°) and intersect both the cap roof (from edge to edge) and the upper boundary of the bubble-depleted region (drawn in the figure with a dashed curve). The intersections—seven for the characteristic length of the cap (h_i) and seven for that of the bubble-depleted region (δ_i)—are then determined to provide the normalized "thickness" of the bubble-depleted region/layer, δ_i/h_i. Two mean values of this thickness are specified—one for the central region ($i = -1$ to 1) and the other for the edge region ($i = \pm 2$ and ± 3)—in order to identify the geometrical deviation of the upper boundary of the bubble-depleted region from the shape of the cap roof. The normalized area of the bubble-depleted region (with the cap area) is also estimated; details of the estimation procedure are given in the appendix.

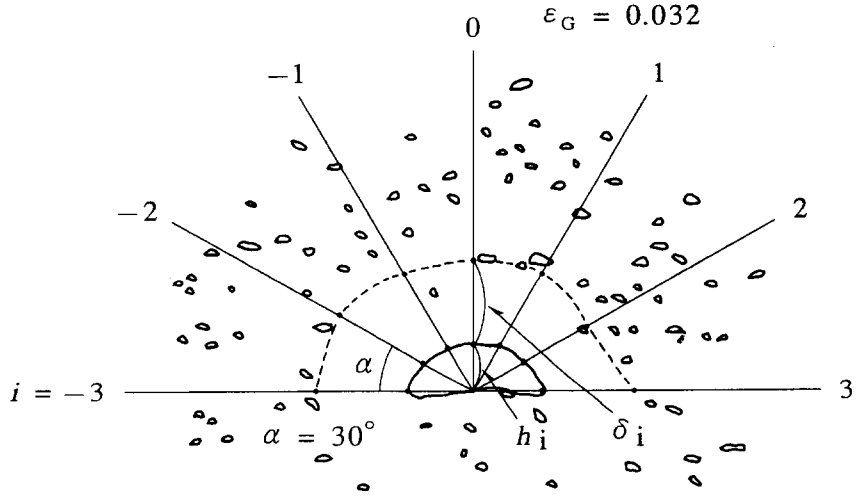

Figure 3. Sketch of the typical redispersed distribution of swarm bubbles in the front vicinity of approaching cap bubble.

Thickness of the bubble-depleted region/layer

Figure 4 shows the variation, with the swarm gas hold-up, of the normalized mean thickness of the bubble-depleted layer (δ/h) near (a) the cap central region and (b) the cap edge region. Each data point is given with the standard deviation, represented in the figure by a vertical line. In both cases, δ/h exhibits a peculiar trend at a (critical) gas hold-up of around $\epsilon_G = 0.01$; it sharply decreases as ϵ_G increases to approach this critical value, gradually decreases afterwards and apparently converges to some asymptotic value of approximately unity. While the standard deviations are large below the critical ϵ_G, they become smaller above it. An important implication of this trend, though not discussed here, is that the extent of the bubble-depleted region may have a very close relationship with that of the cap–bubble interaction; details of this aspect are discussed elsewhere (Tsuchiya *et al.* 1994).

Another point can be noted in figure 4[(b) to be specific] when comparing the two data sets, i.e. the data points (represented by the smooth, partially dashed, solid curve) and the dotted curve [representing the data of figure 4(a)]. While for $\epsilon_G > 0.01$ the two curves almost coincide with each other, the dotted curve (i.e. for δ/h near the cap central region) takes definitely larger values than the solid one (i.e. for δ/h near the cap edge region) for lower ϵ_G. This implies that while the upper boundary of the bubble-depleted region has a shape similar to the cap frontal shape (approximately part of a circle; see appendix) in a bubble swarm of large bubble population, it has a vertically elongated shape (or, in terms of a simpler geometrical interpretation, the representative circle is displaced upwards) in the swarm of ϵ_G below the critical value.

Apparently the only relevant data available in the literature are from Hills (1975). He superimposed on each frame of cine-photography (similar to the sketch in figure 3) a grid comprising three concentric annular spaces of equal area which covered the front vicinity of the cap. By counting the number of bubbles in each annular sector, Hills obtained the mean gas hold-up as a function of radial distance from the center of curvature; the results, after being converted to the characteristic length ratio defined specifically in the present study, are plotted in figure 4(a). Note that Hills' data are provided in terms of the δ/h range corresponding to 50–90% of a given swarm gas hold-up, due to a rather slow transition in the voidage variation across the upper bound of the bubble-depleted region as well as appreciable scattering in his data. As can be seen in the figure, Hills' results roughly coincide with the present results which cover a wider range of the swam gas hold-up.

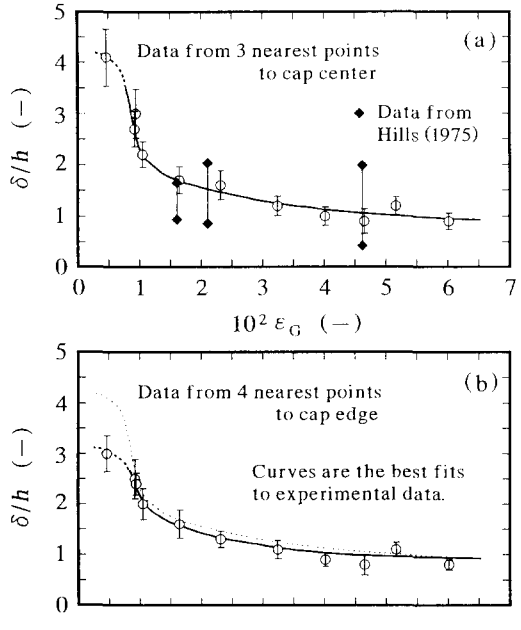

Figure 4. Variation, with swarm gas hold-up, of the normalized thickness of the bubble-depleted region near the cap (a) central and (b) edge regions.

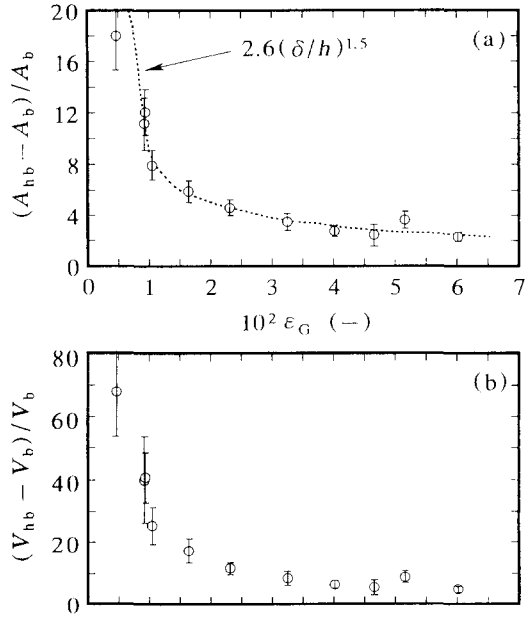

Figure 5. Variations, with swarm gas hold-up, of the normalized (a) area and (b) volume of the bubble-depleted region.

Area of the bubble-depleted region

A plot, similar to that in figure 4(a) or (b), for the normalized area of the bubble-depleted region is shown in figure 5(a). Note the striking similarity between the thickness and the area of the region in their variations with the swarm gas hold-up. In fact, both can be interchanged using the following simple relationship:

$$(A_{hb} - A_b)/A_b = 2.6(\delta/h)^{1.5} \quad [2]$$

for the particular data sets given in figures 4(a) and 5(a), except at the lowest ϵ_G range (below the critical value). Accordingly, a simple, indirect way for evaluating the normalized area of the bubble-depleted region can be established via a relationship such as [2] along with the measurement of only the vertical height of the bubble-depleted region, δ_0 (as well as the bubble height, h_0). Hills (1975) gave only a rough estimate of the area of the bubble-depleted region as being about four times the cap area provided the swarm gas hold-up is $\leqslant 4\%$. This value is just about the average of the present results if the gas hold-up range is fixed at $\epsilon_G = 0.02$–0.04 [see figure 5(a)].

As a complementary result, the normalized volume of the bubble-depleted region "extrapolated" from the present 2-D data (see appendix) is given in figure 5(b). It seems reasonable to have a relatively large uncertainty of the volume—more exaggerated than the thickness or area—estimation for ϵ_G below the critical value due to the relatively vague boundary of the bubble-depleted region; for higher ϵ_G, the error is much smaller so as to give reliable estimates of the relevant volume which has a value of an order of ten times the cap volume. This value, however, needs to be validated through further investigations involving the direct measurement of the dimensions of the bubble-depleted region in a 3-D system. The influence of the narrow gap (i.e. 2-D effect) on the characteristics of the bubble-depleted region is inevitable just as it is for the bubble rise velocity, the gas hold-up or the pressure distribution around the cap. It is only speculated that since the degree of freedom of the bubbles directly ahead of the cap nose to move away from the approaching cap is greater in three dimensions than two dimensions, the extent of the bubble-depleted region in practical 3-D systems could be larger than the estimates obtained in the present 2-D system. From the viewpoint of the difference in the extent of modification of the axial pressure distribution in front of the cap (thus the effective buoyancy acting on the bubbles ahead, as discussed earlier) between the 2-D and 3-D systems, however, such an argument cannot be conclusive unless one measures or estimates (and then compares) the pertinent pressure distributions in both systems.

CONCLUDING REMARKS

An injection of a large cap bubble into a swarm of uniformly distributed small bubbles causes local redispersion of small bubbles around the cap. Confirmed in this study is the formation of a bubble-depleted region/layer right above the cap frontal surface. The extent (height/thickness, area or volume) of this region is found to vary with the swarm gas hold-up in a peculiar way; there exists a critical gas hold-up below which the extent sharply decreases with an increase in the gas hold-up and above which the decreasing rate is much smaller. For a nitrogen–tap water system this critical value is ~ 0.01.

REFERENCES

AKITA, K. & YOSHIDA, F. 1974 Bubble size, interfacial area, and liquid-phase mass transfer coefficient in bubble columns. *Ind. Engng Chem. Proc. Des. Dev.* **13,** 84–91.

CLIFT, R., GRACE, J. R. & WEBER, M. E. 1978 *Bubbles, Drops, and Particles.* Academic Press, New York.

HILLS, J. H. 1975 The rise of a large bubble through a swarm of smaller ones. *Trans. Inst. Chem. Engrs* **53,** 224–233.

HILLS, J. H. & DARTON, R. C. 1976 The rising velocity of a large bubble in a bubble swarm. *Trans. Inst. Chem. Engrs* **54,** 258–264.

MARKS, C. H. 1973 Measurements of the terminal velocity of bubbles rising in a chain. *Trans. ASME, J. Fluid Engng* **95,** 17–22.

MIYAHARA, T. & FAN, L.-S. 1992 Properties of a large bubble in a bubble swarm in a three-phase fluidized bed. *J. Chem. Engng Jpn* **25,** 378–382.

MIYAHARA, T., TSUCHIYA, K. & FAN, L.-S. 1991 Effect of turbulent wake on bubble–bubble interaction in a gas–liquid–solid fluidized bed. *Chem. Engng Sci.* **46,** 2368–2373.

TSUCHIYA, K. & NAKANISHI, O. 1992 Gas holdup behavior in a tall bubble column with perforated plate distributors. *Chem. Engng Sci.* **47,** 3347–3354.

TSUCHIYA, K., OHSAKI, K. & TAGUCHI, K. 1994 Stability of a large bubble rising in a 2-D bubble column with uniform bubbling. *Soc. Chem. Engng Japan Regional Meeting*, Tokushima, Japan, 20–21 July, paper (B23); also to be presented at *2nd Int. Conf. Multiphase Flow*, Kyoto, Japan, 3–7 April (1995).

WALLIS, G. B. 1969 *One-dimensional Two-phase Flow*. McGraw–Hill, New York.

APPENDIX

Figure A1 depicts a geometrical simplification, adopted in this study for estimating the normalized area of the bubble-depleted region, where both the cap frontal surface and the upper bound of this region are to be approximated by circle segments (solid curves). The estimation of the areas below these arcs (and above the horizontal line) starts with finding, on the desired circles, a pair of the optimum co-ordinate sets which correspond to a pair of seven (or occasionally five; $i = -2$ to 2) intersections obtained experimentally, such as the ones given in figure 3. Specific optimization for each arc is carried out by minimizing the following objective function:

$$F(p, q) = \sum_{i=-3}^{3} [p + q - \sqrt{h_i^2 + q^2 - 2h_i q \cos(\pi - i\alpha)}]^2 \qquad [A1]$$

The optimum values of p and q specify the circle radius, i.e. $R = p + q$; half the subtended angle is given by $\cos\theta = q/R$. The circular-cap area is then calculated from

$$A = (R^2/2)(2\theta - \sin 2\theta) \qquad [A2]$$

The same procedure is repeated for the cap and the bubble-depleted region (plus cap) to find their areas, A_b and A_{hb}, and the required area ratio, $(A_{hb} - A_b)/A_b$; here (and in figure A1) the subscripts b and hb stand for the cap bubble itself and the bubble-depleted region (or "hole") and bubble combined, respectively. This approach can be extended to evaluating the volume ratio; a simple way of doing this is to consider a body of revolution about the cap central axis, i.e. a

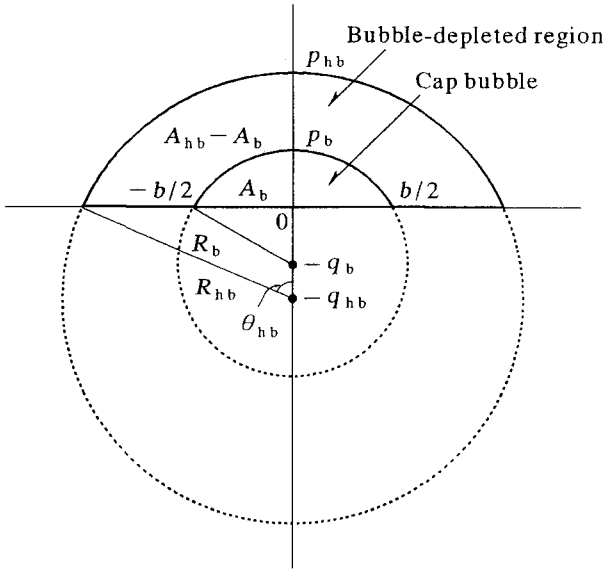

Figure A1. Simplified geometrical configuration of the cap bubble and bubble-depleted region.

spherical cap having a circular-cap projection whose area is given by [A2]. The pertinent volume is then expressed as

$$V = (\pi h^2/3)(3R - h) \qquad [A3]$$

The validity of this simple geometrical assumption depends crucially on whether one accepts the hypothesis that the area obtained in the present 2-D experimentation can truly represent the projection of the 3-D counterpart in practical BCRs. This aspect requires further investigation, i.e. direct measurement of the volume of the bubble-depleted region in a 3-D system, which goes beyond the scope of this communication.